INTL JOURNAL OF ELECTRONICS AND TELECOMMUNICATIONS, 2020, VOL. 66, NO. 1, PP. 201–210
Manuscript received November 15, 2019; revised January, 2020. DOI: 10.24425/ijet.2020.131864

The analysis of energy consumption in 6TiSCH network nodes working in sub-GHz band

Mateusz Kubaszek, Jan Macheta, Łukasz Krzak, Cezary Worek

***Abstract*—The 6TiSCH communication stack enables IPv6 networking over the TSCH (Time Slotted Channel Hopping) mode of operation defined in IEEE 802.15.4. Lately it became an attractive solution for Low power and Lossy Networks (LLNs), suitable for Industrial Internet of Things (IIoT) applications. This article introduces a credible energy consumption model for the 6TiSCH network nodes, operating in the 863-870 MHz band. It presents the analysis leading to the construction of the model as well as verification through experimental measurements which showed 98% accuracy in determining power consumption for two different network topologies. The article includes reliable battery lifetime predictions for transit and leaf nodes along with other parametric study results.**

***Keywords*—IEEE 802.15.4e, TSCH, 6TiSCH, energy modelling, energy consumption, wireless sensor networks, Industrial IoT, mesh networks**

I. Introduction

THE LLNs are essential elements of many Internet of Things (IoT) solutions. They provide low-power wireless connectivity in large deployments involving hundreds or even thousands of devices. The introduction of TSCH technique in LLNs achieved wide recognition, as it provides deterministic operation capabilities, scalability and quality of service desired by the IIoT applications [1], [2]. A wireless communication stack, serving as a building block for such applications, is expected to be Internet-ready by utilising IPv6 protocol and should provide a reliable connection in harsh industrial environments. Moreover, it is expected that such solution will also allow some devices in the network to be battery powered. This is challenging, especially for LLNs optimised for low-cost systems that utilise heavily constrained hardware platforms. Employing TSCH helps to solve many of these issues.

Nodes in TSCH LLNs communicate with each other in a synchronous manner - following a schedule, consisting of transmission, reception, or sleeping slots, that is constructed dynamically based on the network topology and data traffic. Each packet transmission occurs in one of the predefined frequency channels that are changed in a pseudo-random fashion, which mitigates interference-related issues. This technique can be used in various frequency bands, including 2.4GHz and sub-GHz bands, allowing to adapt to the specific system requirements. Since the TSCH slots are allocated prior to their usage, packet collisions are drastically reduced compared to the popular Carrier Sense Multiple Access techniques, allowing high bandwidth utilisation. Finally, TSCH allows to shorten idle listening, resulting in reduced power consumption, which opens the possibility to power the devices from battery or renewable power sources. Moreover, since nodes behave in a deterministic manner, it is possible to construct a credible energy consumption model that can be used to forecast the battery lifetime or even optimise resource allocation and routing to extend the lifetime of the whole network.

This paper presents an accurate analysis of energy consumption in TSCH-enabled nodes, based on an analytical model. The rest of the paper is organised in the following way: chapter II gives an overview of the 6TiSCH communication stack that enables IPv6 networking in TSCH networks, chapter III presents the adaptation of this stack to the 863-870 MHz European radio band, chapters IV and V present the actual energy consumption model along with its experimental verification and chapter VI presents related work. Conclusions and future work is discussed in chapter VII.

II. The 6TiSCH communication stack

One of the first communication protocols engaging TSCH was Time Synchronized Mesh Protocol which demonstrated high reliability level in industrial deployments with the Packet Delivery Ratio (PDR) reaching over 99.9% [3]. TSCH was also used in commercial grade industrial LLN stacks: Wireless-HART and ISA100.11a which operate in the unlicensed 2.4GHz radio band. Later (in 2012) TSCH was brought to the IEEE802.15.4 standard as a new MAC (Media Access Control) layer and soon after (in 2013) the IETF working group called 6TiSCH was formed, to enable the IPv6 protocol to run over the TSCH mode [4]. 6TiSCH merges the 6LoWPAN stack with IEEE802.15.4e-TSCH MAC and Physical (PHY) layers. Even though the problem of effective link layer resource allocation was not completely solved, the 6P/6top framework was introduced [5] which enabled a variety of allocating techniques to be applied. 6TiSCH solved the problem of node association and connection maintenance. Moreover the Minimal Scheduling Function (MSF) was proposed [6] as a simple decentralised allocator that enabled basic communication. 6TiSCH stack is still under standardisation process and is being developed by academic institutions and private companies.

Nodes in the 6TiSCH networks operate according to a schedule and communicate with each other in dedicated cells of following types:

This work was financed by the statutory activity of the AGH University of Science and Technology.

M. Kubaszek, J. Macheta, Ł. Krzak, C. Worek are with AGH University of Science and Technology, Faculty of Computer Science, Electronics and Telecommunications, Department of Electronics, Krakow, Poland (e-mail: kubaszek@agh.edu.pl)

- *Advertising* - Bidirectional cell used for the purpose of joining to the network and parent selection;
- *Managed* - Unidirectional cell used to handle data traffic, has to be negotiated with other node (further on referred to as *Managed up* and *Managed down*);
- *Autonomous* - Unidirectional cell intended for the transmission of packets when no managed cells are allocated. e.g. during association phase (further on referred to as *Autonomous up* and *Autonomous down* cells);

Communication cells are gathered within recurring slotframes. Each cell is described by a slot offset, which indicates position within the slotframe, and a channel offset determining the channel. Association to the network begins with the reception of a Beacon packet which contains Information Elements (IE) required for proper synchronisation with the slotframe. The node then performs a joining process by the preferred Join Proxy node [7] and listens to DODAG Information Object (DIO) packets to select a potential parent. DIOs and Beacons are transmitted periodically over a common advertisement cell. The RPL protocol, through its Objective Function, directs the parent selection for each joining node. Once the parent is properly selected, the node starts sending Destination Advertisement Object (DAO) packets to the DODAG (Destination Oriented Directed Acyclic Graph). In addition, the node is ready to participate in data traffic - it starts sending Beacons, DIOs and data packets. Its parent is the preferred source of synchronisation, so minimal traffic between the two must be maintained to remain synchronised. For this reason short keep alive (KA) packets are sent out when there is no other traffic.

III. 6TiSCH in sub-GHz bands

While the IEEE 802.15.4 250 kbps DSSS-OQPSK-250 PHY is the most commonly used radio interface in LLNs and serves as a reference in the development of the 6TiSCH protocol, in many IIoT applications it suffers from insufficient transmission range, poor obstacle penetration and susceptibility to interference. Fortunately, the 6TiSCH stack can also be used in other frequency bands. In our experiments we have adapted it to the IEEE802.15.4e SUN PHY using the 863-870 MHz band with 69 channels, 100kHz channel bandwidth and 50 kbps FSK. Our 6TiSCH stack implementation is based on the OpenWSN [8] project, developed at the UC Berkeley. This project includes the implementation of all layers of the 6TiSCH stack, that is IEEE802.15.4e MAC, 6P/6top with MSF, RPL ROLL, IPHC and UDP. The stack was ported to a proprietary radio module (timing parameters are presented in Table II) , based on the Silicon Labs EZR32WG330F256R69G microcontroller. It integrates a single ARM Cortex-M4 core with a sub-GHz radio transceiver, following a modern trend in reducing hardware costs. The firmware incorporates event-driven architecture and processes time-critical operations in privileged mode. Lower priority operations are performed in non-preemptive tasks in the background. We have also implemented many modifications including the MAC layer optimisation, so the MCU is woken up only for active slots. As a result, the performance of the MCU is not a significant factor in energy analysis. Table I gathers the most important parameters of the radio module, that were measured during the pre-compliance tests against the relevant ETSI 300 220 standard.

TABLE I
PARAMETERS OF THE RADIO MODULE

Parameter	Value
Sensitivity (15% PER)	-100 dBm
Output power	+13 dBm
Sleep current	1-2 μA
Wakeup time	2 μs
Clock accuracy	± 10 *ppm*
ETSI 300 220 Class	1.5

TABLE II
MAC TIME PARAMETERS

Time parameters (MAC PIB)	Value [μs]
macTsDuration	35009.6621
macTsTxOffset	2120
macTsRxOffset	1560
macTsMaxTx	30000
macTsMaxAck	15000
macTsRxWait	1120
macTsAckWait	500
macTsTxAckDelay	1350
macTsRxAckDelay	1100

IV. Energy consumption model

Having a reliable energy consumption model is crucial for autonomous devices powered from a battery or renewable energy source. Such model can be used to predict battery lifetime but in 6TiSCH network that is not the only use case. While the distributed MSF resource allocation algorithm is the default one, a lot of research was lately done on centralised and decentralised schedulers that operate in the network-wide scale, optimising latency or throughput [9]. A credible energy consumption model would enable the same to be done for the optimisation of node's battery life-time.

Our proposed model consists of three layers. First, the current consumption properties of the underlying hardware is described. Despite the use of a proprietary radio module in our evaluation, the provided generic concept of basic radio activities makes it easy to use this model with any other similar hardware platform. Next, taking into consideration that in the TSCH network all radio activities happen within recurring time slots, the second layer of the model categorises all possible slot types and models their unitary charge cost, based on the properties of the hardware platform. Finally, the third model layer will describes the probability of occurrence of each time slot category, by analysing and modelling the traffic. These probabilities depend mainly on the protocol settings, network topology and data traffic. It is worth to note that all this information, required to effectively use this model can be made available to a centralised scheduler.

A. Characteristics of the hardware platform

Figure 1 presents an exemplary oscillogram of the radio transceiver current consumption during a slot, in which the

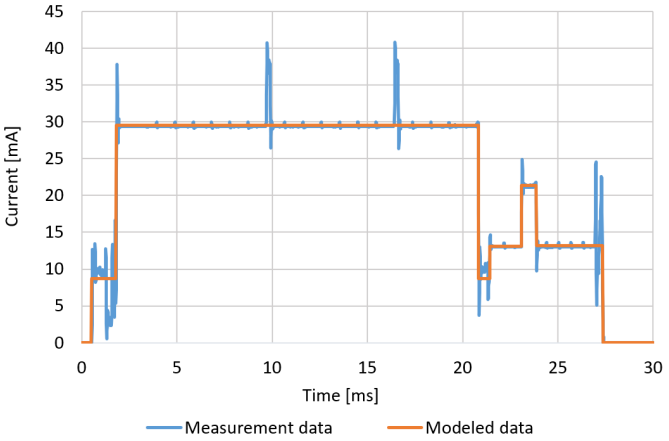

Fig. 1. Exemplary oscillogram showing current consumption of the radio module in a slot where a packet is transmitted and acknowledgement is received.

device transmits a packet and receives acknowledgement. By analysing such oscillograms we have categorised the basic hardware activities, along with their timings and current consumption levels. The results are gathered in Table III, along with other important model parameters. Note that Frame lengths in Table III are given in terms of Physical Protocol Data Unit (PPDU). The parameters cover all possible transceiver activities, while operating in TSCH network. The duration of these activities is implementation-defined, and was empirically fine-tuned during the porting process. Even though the current draw can be taken from the datasheet, experimental evaluation usually results in more precise parametrisation. It is worth noting that, according to our measurements, transmission current has significant impact on the overall power consumption, so special care should be taken when defining it for the model.

The $radioTxRxStartOffset$ parameter is defined as a time difference between the start of transmission and the Start of Frame Delimiter (SFD) recognition. It could be calculated from the length of the transmitted preamble and SFD. However, a particular transceiver may introduce some delay in notifying the stack about ongoing transmission. Therefore the best way is to evaluate this parameter empirically. The $radioTxRxStartOffset$ extends the listening time given by $macTsRxWait$, increasing energy consumption, but it is necessary to determine whether a transmission takes place or not.

B. Slot categorization

The main link layer resource unit in IEEE802.15.4e-TSCH is time slot. In every slot a node can sleep or take part in data exchange by sending or receiving a packet with optional acknowledgement packet (ACK). Table II gathers the MAC timings for a single TSCH slot that were used in the studied implementation for 863-870 MHz band. These parameters have to be the same across all nodes, so certain margins may need to be applied to ensure compatibility with different hardware. Fig. 2 presents the time diagram of a single timeslot

TABLE III
MODEL PARAMETERS

Parameter	Description	Value
T_{TxRx}	radioTxRxStartOffset	1.4 ms
T_{preTx}	radioTxPrepare	1 ms
T_{preRx}	radioRxPrepare	0.8 ms
$T_{preAckTx}$	radioAckTxPrepare	0.55 ms
$T_{preAckRx}$	radioAckRxPrepare	0.45 ms
$T_{startRx}$	radioStartReceiving	0.8 ms
T_{rxw}	macTsRxWait	1.12 ms
T_{ackw}	macTsAckWait	0.5 ms
T_s	macTsDuration	35 ms
I_{sleep}	radioSleepCurrent	2 μA
I_s	radioSynthCurrent	9 mA
I_{listen}	radioListeningCurrent	13 mA
I_{rx}	radioReceivingCurrent	13.5 mA
$I_{rxStart}$	radioStartReceiving	23 mA
I_{tx}	radioTransmitCurrent	36 mA
R	Transceiver Bitrate	50 kbps
L_{ack}	ACK PPDU length	31 B
L_{Beacon}	Beacon PPDU length	51 B
L_{DIO}	DIO PPDU length	101 B
L_{Data}	Data PPDU length	106 B
S	Number of timeslots in slotframe	29

from the perspective of both the transmitter and the receiver, including MCU processing and radio activities. A node may perform one of the following activities within a single slot:

1) *sleep* - transceiver and MCU are in sleep mode. In this case the energy consumed in the slot will be equal to (1).
$$q_{sleep} = I_{sleep} \cdot T_s \tag{1}$$
2) *listening without reception* - radio listens, but no frame is received. In this case the energy consumed in the slot will be equal to (2).
$$q_{listen} = I_{synth} T_{preRx} + I_{listen}(T_{TxRx} + T_{rxw}) \tag{2}$$
3) *broadcast transmission* - frame transmission without receiving ACK. In this case the energy consumed in the slot will be equal to (3),
$$q_{tx}(L) = I_s T_{preTx} + I_{tx}(T_{TxRx} + \frac{8L}{R}) \tag{3}$$
where L is the byte length of the transmitted frame.
4) *broadcast reception* - frame reception without sending ACK. In this case the energy consumed in the slot will be equal to (4),
$$\begin{aligned} q_{rx}(L) = I_s T_{preRx} + I_{listen} \cdot \frac{T_{rxw}}{2} \\ + I_{rx}(T_{TxRx} + \frac{8L}{R}) \\ + T_{startRX}(I_{rxStart} - I_{rx}) \end{aligned} \tag{4}$$
where L is the byte length of the received frame.
5) *unicast acknowledged transmission* - frame transmission and ACK reception. In this case the energy consumed in the slot will be equal to (5),
$$\begin{aligned} q_{txAck}(L) = q_{tx}(L) + I_s T_{preAckRx} \\ + I_{listen} \frac{T_{ackw}}{2} + I_{rx}(T_{TxRx} + \frac{8L_{ack}}{R}) \end{aligned} \tag{5}$$

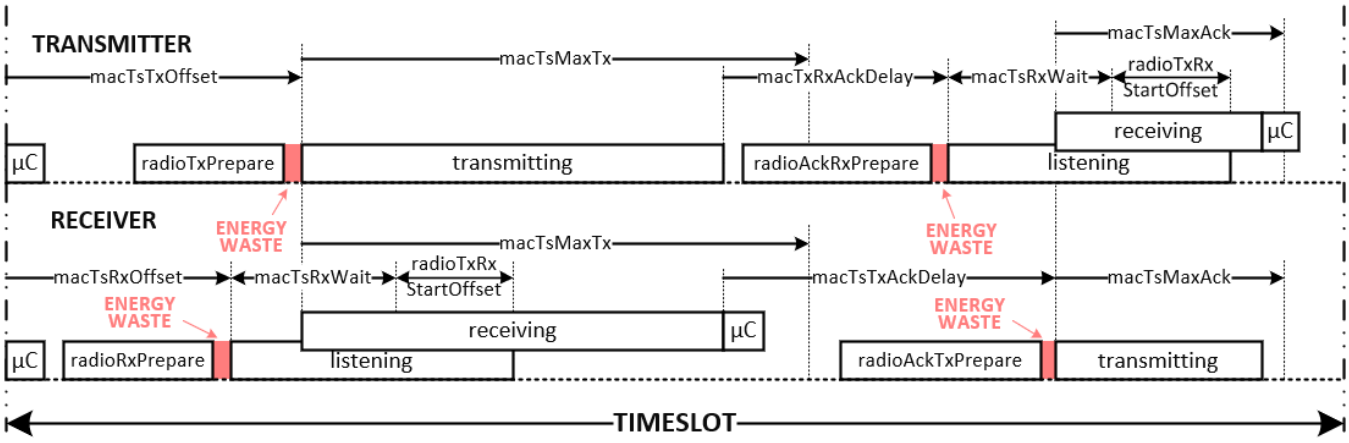

Fig. 2. Slotframe timings including hardware related operations.

where L is the byte length of the transmitted frame and L_{ack} is the byte length of an ACK frame.

6) *unicast non-acknowledged transmission* - frame transmission and listening for ACK, without ACK being sent from other node. In this case the energy consumed in the slot will be equal to (6),

$$q_{txNoAck}(L) = q_{tx}(L) + I_s T_{preAckRx} + I_{listen}(T_{ackw} + T_{TxRx}) \quad (6)$$

where L is the length of the transmitted frame.

7) *unicast reception with acknowledgement* - frame reception and transmission of ACK. In this case the energy consumed in the slot will be equal to (7),

$$q_{rxAck}(L) = q_{rx}(L) + I_s T_{preAckTx} + I_{tx}(T_{TxRx} + \frac{8L_{ack}}{R}) \quad (7)$$

where L is the byte length of the received frame.

8) *unicast reception with no acknowledgement* - the energy consumed in this slot will be the same as in the case of broadcast reception;

Fig. 3 presents the unitary charge consumption associated with each slot type, and distribution of charge between elementary radio activities, given that data frames are 106 B long, and the acknowledgements are 31 B.

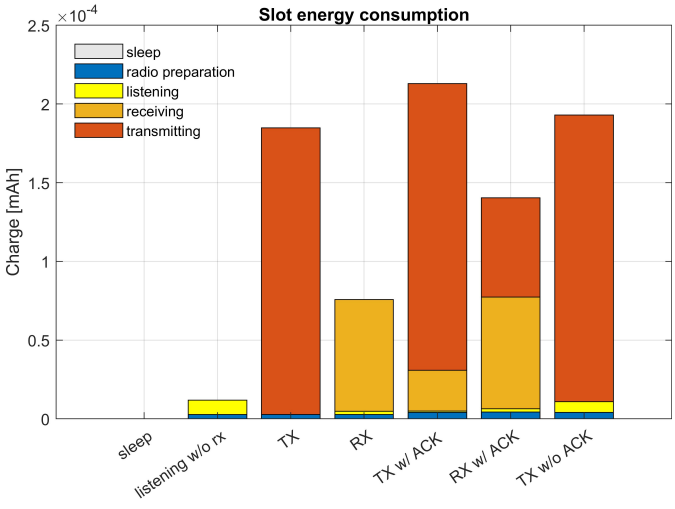

Fig. 3. Unitary charge consumption of possible slot types with additional division into elementary radio module activities.

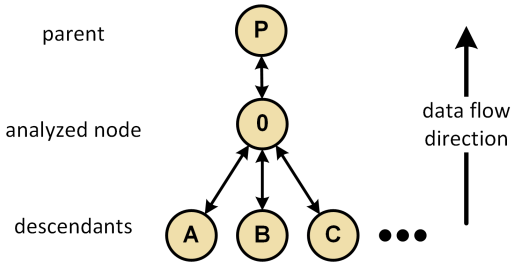

Fig. 4. Visualisation of the topology and traffic model.

C. Cell traffic model

Nodes periodically exchange Advertising messages, i.e. DIO and Beacon packets, that are proprietary to the stack. Every node has to allocate an *Advertising cell*, however the 6TiSCH standard allows a node not to send DIO and Beacons - such node then becomes a leaf node, meaning it may not be connected to any other node, except its parent (transit node).

The 6TiSCH network organises network into DODAG, therefore our model assumes that the analysed node will have a single parent and N children, where $N = 0$ for leaf nodes and $N \geq 0$ for transit nodes, as presented in Fig 4. N.B. a node may be part of many DODAGs, however the presented model does not cover such scenarios.

The application data traffic model assumes that multipoint to point traffic is dominant, what stands true in most sensing applications. 6TiSCH incorporates RPL ROLL routing algorithm with non-storing mode of operation, thus the traffic downward the network is using source routing. In that case the RPL router node serves both as a network coordinator and a border router. We assume that each node allocates unidirectional *managed*

cell to its parent for application data traffic. We further assume that the data can not be aggregated, and every packet received from the descendants must be forwarder towards the border router. Leaf node does not allocate autonomous down cell, because no descendants are foresaw. As a result, the transit node allocates $4 + N$ of active cells, one *advertising*, two *autonomous*, one *managed up* to its parent and one *managed down* for every descendant. Leaf node has always 3 active cells: *advertising*, *autonomous up*, and *managed up*.

The 6TiSCH Network uses keep-alive mechanism that maintains minimal packet exchange rate preventing the node from being desynchronized. However, in our model we assume a typical scenario, that the application-related traffic is enough to maintain the synchronisation and no special KA packets are necessary. Thus our model model takes into consideration transmission and reception of DIO, Beacon and data packets, where the collisions are only considered for the DIO and Beacon packets, since these are carried through the shared advertising slots. In addition the model is parametrised by the PDR for each link, so that the energy related to retransmissions is also taken into account. The 6P/6top packet exchanges were not taken into consideration due to once-in-a-lifetime nature of these transactions in a quasi-static topology. Moreover, RPL DAO packets are also omitted because of the prolonged transmission period (trickle timer).

For the purpose of validation, it is arbitrarily assumed that slotframe has a length of 29 time slots, which gives a slotframe interval of about 1 second. The rest of the basic stack configuration parameters are gathered in Table IV.

We can now model the actual traffic and energy in each of the cell types.

1) Advertising cell: The advertising cells are shared between all networked nodes and used for broadcasting the Beacon and DIO packets. These cells are then naturally prone to packet collision effects. To avoid excessive collision rate a simple mechanism was proposed in 6TiSCH that tries to maintain a fixed cell usage - that is the probability $p_{AdvBusy}$ of Beacon or DIO packet occurrence in an advertising cell. The desired value of this probability is generally application specific, but our experiments have shown that a value of $\frac{1}{3}$ is a good trade-off between the number of collisions and network consistency. In order to reach this probability, in each advertising cell, each node n generates the Beacon and DIO packets alternately with a process governed by a Bernoulli trial and probability given by (8),

$$p_n = \frac{p_{AdvBusy}}{2 \cdot (N_n + 1)} \tag{8}$$

where is the number of descendants of the n-th node and factor 2 stands for the fact that it's either Beacon or DIO that is being sent. Of course such a simple mechanism does not always lead to the desired advertising cell usage. In heavily non-uniform and degenerated topologies, where number of neighbours differ vastly from node to node, this method will need improvement, however in most cases the actual cell usage probability can be approximated by the desired one ($p_{AdvBusy}$).The collision probability in the advertising cell is given by (9), taking into consideration that the individual packet transmissions from each node are independent events.

$$p_{AdvColl,n} = 1 - \prod_{n=1}^{N_n} (1 - 2 \cdot p_n) \tag{9}$$

Our model assumes that there is no way of knowing whether the collision occurred or not, until the whole packet is collected at the receiver and it's integrity is checked (through the checksum field). Therefore the mean energy consumption associated with such an event will be the same as energy consumed when receiving a packet of an average size $(L_{Beacon} + L_{DIO})/2$.

Equation (10) describes the mean charge consumed in the advertising slot of the $n-th$ node. The first two components of the sum represent the case when Beacon and DIO packets are sent in the slot (with probability p_n), the third and fourth component represents the case when Beacon and DIO packets are received and collision occurs, the fifth component represents the case of a collision and the sixth component represents the case when during the advertising slot there was no packet sent.

$$\begin{aligned} q_{Adv,n} &= p_n \cdot q_{tx}(L_{Beacon}) + p_n \cdot q_{tx}(L_{DIO}) \\ &+ (\frac{p_{AdvBusy}}{2} - p_{AdvColl,n}) \cdot q_{Rx}(L_{Beacon}) \\ &+ (\frac{p_{AdvBusy}}{2} - p_{AdvColl,n}) \cdot q_{Rx}(L_{DIO}) \\ &+ p_{AdvColl,n} \cdot q_{Rx}(\frac{L_{Beacon} + L_{DIO}}{2}) \\ &+ (1 - 2p_n - p_{AdvBusy} + p_{AdvColl,n}) \cdot q_{Listening} \end{aligned} \tag{10}$$

2) Autonomous cells: The 6P/6top packets are initially sent through autonomous cells and the same is with any other packet that can not be sent through the dedicated managed cell. Autonomous cell activity is covered by the model but 6P/6top transactions are not taken into account as it was mentioned earlier. Thus the charge consumption in both the up and down cells is modelled as idle listening.

$$q_{AutoUp} = q_{AutoDown} = q_{listen} \tag{11}$$

3) Managed cells: The model takes into account retransmissions caused by non-ideal PDR. The packet error probability is given by $1 - PDR$. Nodes perform up to K retransmissions and the probability of packet being forwarded in $K + 1$ tries is thus given by (12).

$$p_F = 1 - (1 - PDR)^{K+1} \tag{12}$$

As a result, formula (13) describes the factor by which the effective number of data transmissions increases, due to retransmissions, which leads to increased charge consumption.

$$t_K = \sum_{k=1}^{K+1} (1 - PDR)^{k-1} \tag{13}$$

Note that every unsuccessful packet transmission means that no ACK is transmitted back, thus the energy consumption in the packet receiver in the incident slot is lower than in the case of valid packet reception. In further analysis the number of possible retransmissions was set to $K = 3$.

TABLE IV
STACK CONFIGURATION PARAMETERS

Time slots count in slotframe	29
Slotframe interval	1015.28ms
Mean Beacon sending interval	Every sixth slotframe
Mean DIO sending interval	Every sixth slotframe
Mean data sending interval	10s
Descendants count	3

Charge consumed by managed cells consists of the charge consumed in the transmission cell to node's parent and the charge consumed by N_n receive cells, through which data from children nodes are received, as stated in (14).

$$q_{Managed,n}(L) = q_{Parent}(L) + N_n q_{Child}(L) \tag{14}$$

During the managed transmission cell, each node sends data frames if it has them in queue. Otherwise the node remains inactive. We assume, that every child produces new data packet in a slot frame with the probability of p_data and sends it to its parent, but the probability of successful delivery is p_F. The count of frames that are properly delivered to node's parent is also reduced due to p_F, and the overall transmission attempts are increased by a factor of t_K, but with no acknowledges. Thus the charge consumed in the managed cell from $n-th$ node to it's parent is given by (15),

$$\begin{aligned} q_{parent,n}(L) = N_n \cdot p_{data} \cdot \\ (p_F \cdot q_{txAck}(L) + (t_K - 1) \cdot q_{txNoAck}(L)) \end{aligned} \tag{15}$$

where L is the mean Data PPDU length. Similarly, equation (16) express the charge consumed in a cell dedicated for communication with a child. Additional component in the sum is responsible for the case when the child has no data to send, but the node still needs to listen.

$$\begin{aligned} q_{Child}(L) = p_{Data}(p_F \cdot q_{rxAck}(L) \\ +(t_K - 1) \cdot q_{rx}(L)) + (1 - p_{data}) q_{listen} \end{aligned} \tag{16}$$

The final mean energy consumption per slot frame in $n-th$ node $q_{sf,n}$ is qiven as a sum of abovementioned components (17),

$$q_{sf,n} = q_{Adv,n} + q_{AutoUp} + q_{AutoDown} + q_{Managed,n} + S \cdot q_{sleep} \tag{17}$$

and thus the total node's charge consumption in time can be approximated as follows:

$$Q_n(t) \approx \frac{t}{S \cdot T_s} \cdot q_{sf,n} \tag{18}$$

An additional explanation is necessary concerning the KA traffic. The KA packets are sent, when no other packets to which child nodes can synchronise (such as Beacons and DIOs) are present. The minimum KA packet generation period depends in most cases on the hardware-related clock drift. However in most applications the Beacon/DIO traffic is sufficient to keep the nodes synchronised to an acceptable degree, thus the KA packets were omitted in our model. Moreover an additional time synchronisation mechanism may be applied in the form of drift prediction and correction [10]. In our experiments, the KA traffic was only needed if the quiet period in the network reached above 100 seconds.

V. EXPERIMENTAL RESULTS AND MODEL ACCURACY VERIFICATION

The presented model has been verified using a physical network with the nodes that were based on the described proprietary hardware platform. The first topology used to verify the model for transit node consisted of 5 nodes, connected as presented in Fig 4. The second, consisting of a root and a leaf node, was used to verify the model for the leaf node. In both cases, the profiled nodes were powered through a Keysight N6705C power analyser with the N6781A Measure Unit for Battery Drain Analysis, capable of precise current measurement ($104\mu s$ current sampling period with auto-ranging option). A 10-hour long current consumption waveform was gathered for the analysed nodes. Based on that data we were able to describe the node behaviour and the resulting charge consumption in statistical terms and compare the model with the experimental results. It is worth noting that during the experiment the PDR in all links was exactly 100% meaning that not a single data packet transmission in the managed cells failed.

A. Statistical analysis of charge consumption in slots

Since the main transactions that significantly contribute to the overall energy consumption are sending and receiving Beacon, DIO and data packets, we can narrow down the analysed slot types to the following cases:

- transmission of Beacon packet;
- transmission of DIO packet;
- reception of Beacon packet;
- reception of DIO packet;
- transmission DATA packet and receiving ACK;
- reception of DATA packet and sending ACK;

plus additional case, when the node listens but no packet is sent, which happens in the advertising slots. Based on the gathered experimental data, we extracted the charge consumption associated with each of these slot types. The results are shown in Fig. 5. It presents the histograms of charge consumption broken down into the above-mentioned slot types. From each of the histograms we have calculated the expected value and the standard deviation, and compared it to the values predicted by our model. The results are gathered in Table V.

Cases (a), (b), (c) are reception or listening cells and their standard deviation is relatively small. Two distinct spikes in histograms (d), (e) are the result of non-uniform current consumption when the transceiver is transmitting in different channels. This effect is also responsible for the stretching of the right-handed tail in cases (f) and (g). Beacons and DIOs were transmitted on channels 0, 30 and 68 as opposed to DATA packets, which may use any of the available channels. Table VI

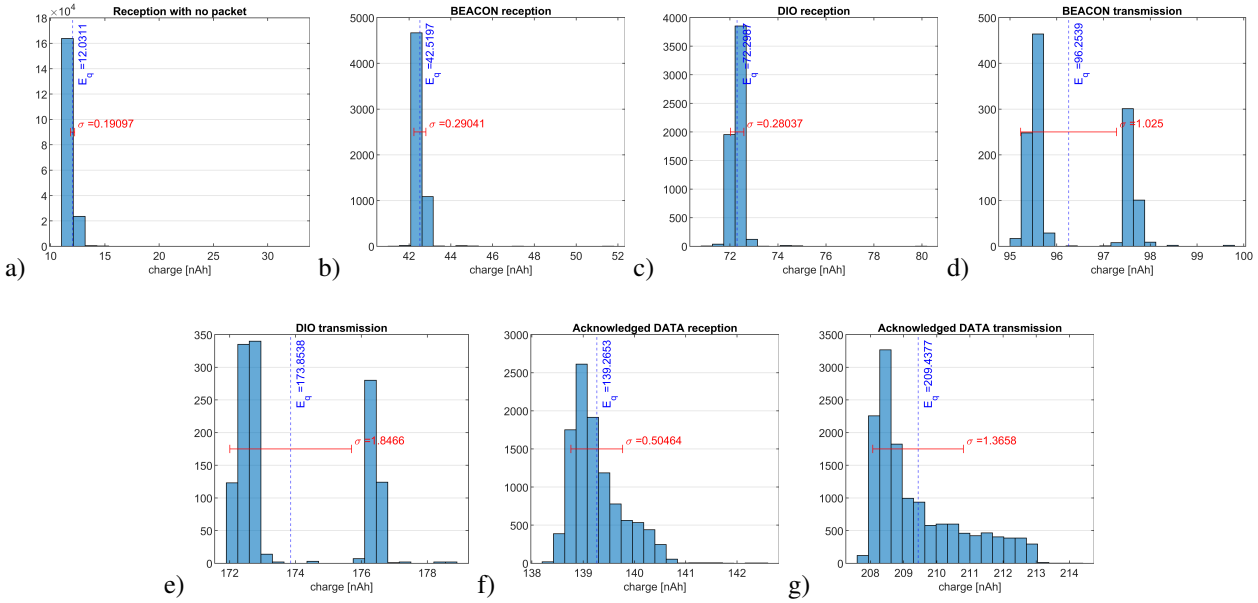

Fig. 5. Histograms of power consumption of respective cell activities. Generated on the basis of 10h current consumption measurement.

TABLE V
VERIFICATION OF CELL CHARGE CONSUMPTION
(CHARGE VALUES IN MAH)

Cell activity	Model charge	Measured mean charge	Measured STDEV	Relative error
Transmission of Beacon	9.76E-05	9.63E-05	1.03E-06	-1.40%
Transmission of DIO	1.77E-04	1.74E-04	1.85E-06	-1.81%
Reception of Beacon	4.28E-05	4.25E-05	2.90E-07	-0.66%
Reception of DIO	7.28E-05	7.23E-05	2.80E-07	-0.69%
Transmission of data (with ACK)	2.13E-04	2.09E-04	1.37E-06	-1.70%
Reception of data (with ACK)	1.40E-04	1.39E-04	5.05E-07	-0.53%
Listen w/o reception	1.19E-05	1.20E-05	2.03E-07	1.09%

explains the above case. Differences in power consumption during transmission mostly depend on the antenna type, RF circuitry and power amplifier type. In our case, the antenna input matching was the reason (we used LINX ANT-868-CW-HWR with 22x31cm ground plane). When terminating the RF output of the radio module the difference in current consumption across all channels was negligible.

The relative error of the presented model does not exceed 2%. The calculated standard deviation values for given slot types are smaller than 2 nAh (less than 1% of mean value), which justifies the use of mean current value as a model parameter, however the model precision could be further refined by including the above-mentioned dependency between current consumption and channel number. Overall the results show that the charge consumed in the transmission and reception slots is highly predictable - as expected in a deterministic communication protocol. Thus the model based on that assumption may be highly accurate.

TABLE VI
TRANSMIT CURRENT VS CHANNEL

Channel	Current [mA]
0	36.45
10	36.1
20	35.8
30	35.6
40	35.5
50	35.4
60	35.4
69	35.5
Max diff.	1.05
Average	35.72

B. *Cell traffic verification*

Since our model is based on the prediction of traffic in the advertising, autonomous and managed cells, we have compared the predicted number of packet transmissions and receptions with the experimental data. Table VII gathers the results for the transit node and Table VIII presents the results for leaf node. The relative error between model predictions and actual results does not exceed 3%. One interesting thing to note here is the dependency between overall node charge consumption Beacon and DIO collision probability, which is very low. In our extended experiments we were able to provoke the nodes to increase the collision rate in advertising channel, however the impact on the charge consumption was insignificant. This is due to the fact, that the charge required to handle a slot in which a packet is received correctly and a slot in which the packet collision occurs is pretty much the

same, since in either case the listening time is similar and the acknowledgements are never sent. Note that within a slot the 6TiSCH implementation does not use any collision avoidance mechanisms.

TABLE VII
CELL TRAFFIC VERIFICATION, TRANSIT NODE.

	Model value	Measured value	Relative error [%]
Beacon sent	1200	1183	1.44 %
DIO sent	1200	1235	-2.83 %
Beacon received	5833	5800	0.75 %
DIO received	5833	5998	-2.75 %
Data packets transmitted	14400	14008	2.80 %
Data packets received	10800	10513	2.73 %

TABLE VIII
BEHAVIOURAL TEST RESULTS, LEAF NODE.

	Model value	Measured value	Relative error [%]
Beacon received	5833	5830	2.92 %
DIO received	5833	6068	-1.12 %
Data transmitted	3600	3509	2.59 %

C. Verification of battery lifetime prediction

Table IX shows operation time of a transit and a leaf node as measured empirically and predicted by the model. We can see that these two scenarios present extremely different use cases - the leaf node, unlike the transit node, has no descendants so it maintains only one connection to its parent. Relative error of 1.37% for the transit node and 1.01% for the leaf node proves the credibility of the model. To our knowledge the small surplus of operation time calculated by the model may be contributed by the activity of MCU not related to radio transmission aspects. Moreover some inaccuracies in radio, cell and behavioural model discussed above have an undeniable influence on the final result.

TABLE IX
VERIFICATION OF NODE LIFETIME PREDICTIONS

Parameter	Transit node	Leaf node
Average current [mA]	0.782	0.220
Days of operation per ampere-hour [day/Ah]	53.3	189.7
Modelled days of operation per ampere-hour [day/Ah]	54.0	191.6
Relative error	1.37 %	1.01 %

D. Other model predictions

Since the model is parametrised with a PDR, we can make predictions for low channel quality conditions. Exemplary model predictions are shown in Fig. 6 for transit node and Fig. 7 for leaf node. They show the working time in days on a unitary 1Ah charge at two arbitrarily chosen PDR rates. Fig. 6 (a) presents the lifetime of a node in relation to the number its descendants, assuming that every child node sends data packet with an average period of 10 seconds. With the assumed slotframe of 29 slots, the 23 descendant nodes is an extreme case making the parent link fully utilised. In this situation, node will allocate additional slots to its parent in advance so that traffic can get by the link between the nodes. This graph stops at a value representing all slots being occupied (1 adv cell, 2 autonomous cells, 3 parent cell, 23 child cells; sum of them equals 29). Fig. 6 (b) shows the dependency between the expected operating time and the period of DATA packet generation among all the descendants. Extending the transmission period will effectively turn more receiving slots into listening slots. The leaf node, as expected, presents much better lifetime capabilities. The operating time of such node may be significantly extended if it does not participate in packet forwarding. As presented in Fig. 7 (a), the reduction of the packet sending period above a certain limit does not significantly change its expected lifetime. Fig. 7 (b) shows that the lifetime highly depends on the slotframe size. Increasing slotframe length reduces the advertising channel duty cycle, so the battery life can be extended. This justifies the use of a multiple overlapping slotframes within a single network when there is a need for battery-powered devices with low bandwidth requirements. The presented predictions however were not verified by practical experiment yet - they serve as an illustration of what kind of predictions are possible using the presented model. Validation of these is planned as our future work.

VI. RELATED WORK

In the literature the topic of energy modelling is discussed in many contexts. An acute insight in transceiver energy modelling is presented in [11] where the energy model was introduced, taking into account the diagram of working states of typical transceivers. In our solution, the demands of upper layer are already defined, therefore we have generalised the operation of the radio in the context of TSCH. [12] presents an example of a node in context of a wireless application for a ZigBee network going into the details of packets collisions and its impact on the power consumption. Topic similar to our own work has also been presented in [13] where an apposite model of activities of TSCH node has been proposed. However this analysis was carried out for TSCH operation in 2.4GHz band. An interesting comparison of TSCH and alternative configuration of the link layer is presented in [14] which merges a generalised energy consumption model with few behavioural scenarios. [15] shows the evaluation of energy in 868MHz band and draw conclusions about the differences in the energy of a network operation. In this article we provide additional supplementation to the energy model in the form of introduction of autonomous cells. Moreover, a long-term verification measurement with a statistical approach is presented.

VII. CONCLUSION

The article presents a deeper analysis of energy consumption in 6TiSCH nodes, that use the TSCH slot-based mode

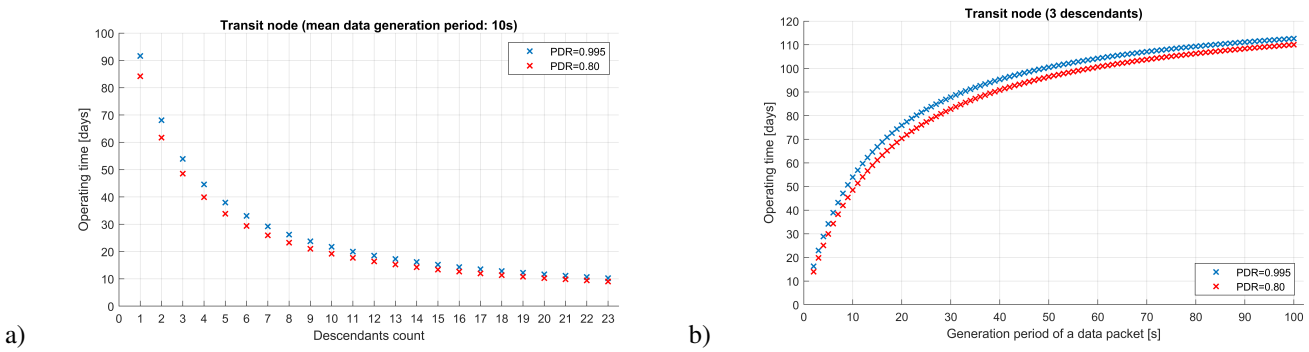

Fig. 6. Model predictions on the operating time for transit node: (a) as a function of the number of descendants, (b) as a function of DATA packet generation period.

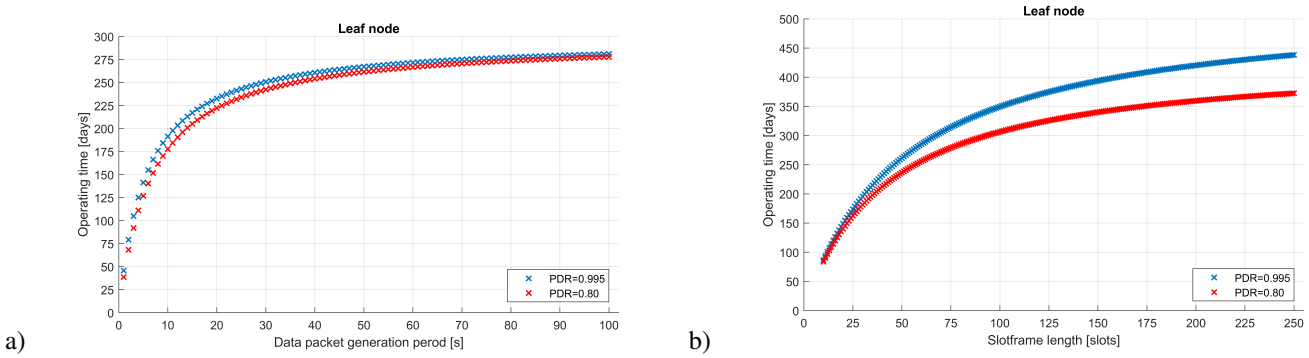

Fig. 7. Model predictions on the operating time for leaf node: (a) as a function of DATA packet generation period, (b) as a function of slotframe length.

of communication. The results are presented for a proprietary sub-GHz 863-870MHz PHY, that is an attractive alternative to the popular 2.4GHz PHYs, especially in the context of IIoT applications. However, with a minimal effort the model can be adopted to any other compatible hardware platform. Based on the generic modelling of current consumption related to basic transceiver operations, the analysis of possible slot types and modelling of traffic within these slots we present a flexible model that can reliably predict the charge consumption of both the transit and leaf nodes in various network topologies. The model was verified through experimental, 10 hour long network operation, where the current consumption of nodes under test was precisely measured. The results show that the network operation is deterministic and our model is credible, reaching an accuracy of more than 97%. One interesting feature of the 6TiSCH stack, that was confirmed in the model and our experiments was the straight correlation between generated packet traffic and energy consumption. The employed slot allocation mechanisms based on TSCH technique led to congestion-free network operation. In a 6TiSCH network collisions occur generally only in the advertising slots, and even there their contribution to the overall energy consumption is insignificant. The presented energy consumption modelling can be used in two forms. First of all, the model can be used to estimate the lifetime of battery-powered devices or the capabilities of renewable power sources required to power such devices. Secondly, due to it's low-complex nature it can be integrated with a centralised 6TiSCH scheduler to introduce the expected operation time metric of battery-powered nodes to the RPL ROLL objective function. Thanks to such a mechanism, the traffic could be routed between the nodes e.g. to even out the energy consumption in the whole network.

REFERENCES

[1] T. Watteyne, A. Mehta, K. Pister, "Reliability Through Frequency Diversity: Why Channel Hopping Makes Sense", in Proc. ACM Symposium on Performance evaluation of wireless ad hoc, sensor, and ubiquitous networks (PEWASUN), Tenerife, 2009, p. 116–123

[2] R. Alves and C. B. Margi, "IEEE 802.15.4e TSCH mode performance analysis", in Proc. of the IEEE 13th International Conference on Mobile Ad Hoc and Sensor Systems (MASS), Brasilia, 2016, pp. 361-362.

[3] K. S. J. Pister and L. Doherty, "TSMP: Time synchronized mesh protocol", in Proc. of IASTED International Symposium Distributed Sensor Networks, Orlando, 2008, pp. 391-398.

[4] X. Vilajosana, Ed., K. Pister,and T. Watteyne, "Minimal IPv6 over the TSCH Mode of IEEE 802.15.4e (6TiSCH) Configuration", BCP 210, RFC 8180, DOI 10.17487/RFC8180, May 2017.

[5] Q. Wang, Ed, X. Vilajosana and T. Watteyne, "6TiSCH Operation Sublayer (6top) Protocol (6P)", RFC 8480, DOI 10.17487/RFC8480, November 2018

[6] T. Chang, Ed., M. Vucinic, X. Vilajosana, S. Duquennoy and D. Dujovne, "6TiSCH Minimal Scheduling Function (MSF)", online, available: https://tools.ietf.org/pdf/draft-ietf-6tisch-msf-08.pdf

[7] M. Vucinic, Ed., J. Simon, K. Pister and M. Richardson, "Minimal Security Framework for 6TiSCH", online, available: https://tools.ietf.org/pdf/draft-ietf-6tisch-minimal-security-13.pdf

[8] T. Watteyne, X. Vilajosana, B. Kerkez, F. Chraim, K. Weekly, Q. Wang, S. Glaser and K. Pister, "OpenWSN: a standards-based low-power wireless development environment", *TRANSACTIONS ON EMERGING TELECOMMUNICATIONS TECHNOLOGIES*, 2012, pp. 480-493.

[9] R. T. Hermeto, A. Gallais and F. Theoleyre, "Scheduling for IEEE802.15.4-TSCH and Slow Channel Hopping MAC in Low Power Industrial Wireless Networks: A Survey", Computer Communications, vol. 114, pp. 84-105, Dec. 2017.

[10] D. Stanislowski, X. Vilajosana, Q. Wang, T. Watteyne, and K. Pister, "Adaptive Synchronization in IEEE802.15.4e Networks", IEEE Transactions on Industrial Informatics, vol. 10, no. 1, pp. 795–802, Feb. 2014.

[11] Q. Wang and W. Yang, "Energy Consumption Model for Power Management in Wireless Sensor Networks", presented at 4th Annual IEEE Communications Society Conference on Sensor, Mesh and Ad Hoc Communications and Networks, San Diego, June 18-21, 2007, 10.1109/SAHCN.2007.4292826.

[12] E. Casilari-Perez, J. M. Cano-García and G. Campos-Garrido, "Modeling of current consumption in 802.15.4/ZigBee sensor motes", Sensors, Basel, 2010.

[13] X. Vilajosana, Q. Wang, F. Chraim, T. Watteyne, T. Chang and K. S. J. Pister, "A Realistic Energy Consumption Model for TSCH Networks", IEEE SENSORS JOURNAL, vol. 14, no. 2, pp. 482-489, Feb. 2014.

[14] I. Juc, O. Alphand, R. Guizzetti, M. Favre and A. Duda, "Energy consumption and performance of IEEE 802.15.4e TSCH and DSME", in Proc. of the IEEE Wireless Communications and Networking Conference (WCNC), Doha, 2016.

[15] G. Daneels, E. Municio, B. V. de Velde, G. Ergeerts, M. Weyn, S. Latré and J. Famaey, "Accurate Energy Consumption Modeling of IEEE 802.15.4e TSCH Using Dual-Band OpenMote Hardware", Sensors, Basel, 2018.